Ultra-compact eight-channel silicon wavelength demultiplexer via digitized meta-structure

Rui Wu
School of Information Science and Engineering
Yanshan University
Qinhuangdao, China
wurui@stumail.ysu.edu.cn

Fengyao Ding
School of Information Science and Engineering
Yanshan University
Qinhuangdao, China
3318447020@qq.com

Boai Liu
School of Information Science and Engineering
Yanshan University
Qinhuangdao, China
1139345591@qq.com

Yingjie Liu
School of Information Science and Engineering
Yanshan University
Qinhuangdao, China
liuyingjie@ysu.edu.cn

Ke Xu
Dept. of Electronic and Information Engineering
Harbin Institute of Technology
Shenzhen, China
kxu@hit.edu.cn

***Abstract*—An ultra-compact eight-channel wavelength demultiplexer with 20 nm spacing and a footprint of 7.2×12 μm² is designed via digitized meta-structure. The simulation peak insertion loss is 2.2 dB, and the crosstalk is <-10 dB.**

Keywords—silicon photonics, wavelength demultiplexer, inverse design

I. Introduction

The exponential growth of big data applications and cloud services demands that the data capacity of the internet infrastructure must be significantly increased. The wavelength division multiplexing (WDM) system can expand the communication capacity and improve the data transmission rate, which plays a significant role in optical interconnection, optical switching and quantum technologies. Wavelength (de)multiplexer is an important component in WDM system, which is used to separate and combine different wavelength signals. Conventional on-chip photonic integrated devices used for wavelength (de)multiplexing include arrayed waveguide grating (AWG) [1], Mach-Zehnder interferometer (MZI) [2, 3], micro-ring resonator (MRR) [4], subwavelength grating (SWG) [5]. These devices have been reported relatively mature mechanisms and design methods, which can achieve wavelength (de)multiplexing with more dense wavelength spacing and more channels. However, it takes a long time to manually design and optimize the structure parameters, and the device size is relatively large, which affects the WDM system integration.

With the demand for the compact integration of on-chip photonic devices, a digitized meta-structure based on inverse design is proposed to reduce the footprint and avoid design obstacles due to the lack of known underlying mechanisms, which has recently shown great potential to create novel functionalities [6-13]. Several wavelength demultiplexers based on meta-structure have been reported [9-13]. For example, A. Y. Piggott et al. experimentally demonstrated a silicon wavelength demultiplexer with 2.8×2.8 μm² footprint that splits 1300 nm and 1550 nm [9]. J. B. Yang et al. proposed a tunable four-channel wavelength demultiplexer with ~62 nm channel spacing and a footprint of only 2.4×8.4 μm² using an objective-first algorithm [13]. It can be seen that the footprint of device is reduced by more than one order of magnitude compared with conventional wavelength demultiplexers, but the device still has limited channels (<4) and larger channel spacing (>40 nm).

In this paper, an ultra-compact wavelength demultiplexer is designed based on digitized meta-structure. The 8 channel and 20 nm channel spacing can be realized within only a footprint of 7.2×12 μm² by a sophisticatedly engineered refractive index profile using the inverse design method. We numerically simulate the transmission properties of the designed device, and theoretically analyze the fabrication and temperature tolerance of the device. All indicate the good performance of our wavelength demultiplexer.

II. Device Design

The eight-channel wavelength demultiplexer is designed on silicon-on-insulator (SOI) platform with single fully etched 220 nm thick Si layer and SiO_2 cladding. The 3D schematic diagram of the device is illustrated in Fig. 1(a). The widths of the input and output waveguide are chosen to be 0.5 μm in order to ensure TE_0 fundamental mode. The gap

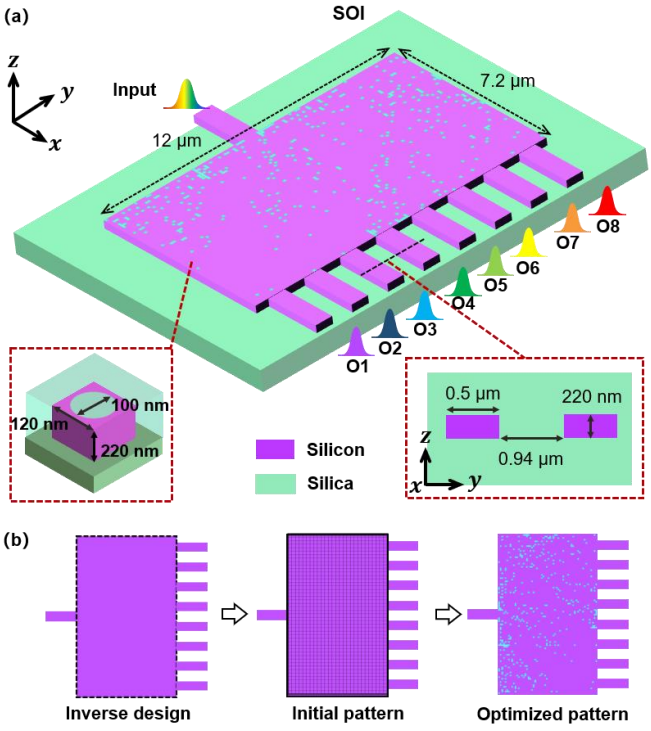

Fig. 1. (a) The 3D schematic structure of the designed eight-channel wavelength demultiplexer via digitized meta-structure. (b) The inverse-design process.

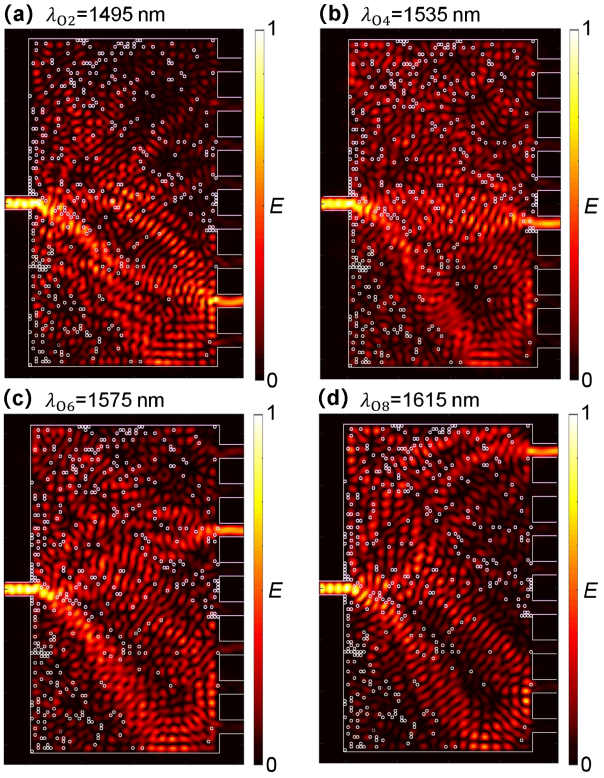

Fig. 2. The simulated optical field distribution of the optimized wavelength demultiplexer at (a) 1495 nm, (b) 1535 nm, (c) 1575 nm, (d) 1615 nm, respectively.

of output waveguide array is defined as 0.94 μm to avoid channel crosstalk. The inverse-design process is sown in Fig. 1(b). The inverse-design region is a rectangle with 12×7.2 μm^2 footprint, which is divide into 120×60 pixels. Each pixel is a square of 120×120 nm^2 with a 100 nm-diameter and 220 nm-depth nanohole. The material property of each hole can be Si or SiO_2. For the initial model, all the holes are set to Si material. The profile of digitized meta-structure is optimized using the direct binary search (DBS) method. The design target can be described by a figure of merit (FOM) which is defined as:

$$FOM = \frac{1}{8}\sum |\alpha_i t_i| \quad (1)$$

where i is the i-th wavelength channel (i=1,2,…,8), t_i is the transmission efficiency of the i-th channel, α_i is weight coefficient of the i-th channel, which is used to optimize the transmission uniformity of different output channels. The modal and FOM are calculated via the three-dimensional finite difference time domain (3D FDTD) method by using Lumerical FDTD solution software. The design process is completed for several iterations until the objective is met or the FOM is not improved further.

III. Device Simulation And Discussion

To evaluate the performance of the optimized wavelength demultiplexer, the optical field distribution at the different operating wavelengths is numerically calculated using 3D FDTD simulation. Fig. 2(a)-(d) show simulation results at four operating wavelengths (1495 nm, 1535 nm, 1575 nm and 1615 nm). It can be seen clearly that most of the light is propagating efficiently following the designed pathway, and negligible beam distortion or radiation leakage is observed. The transmission spectra of the designed wavelength

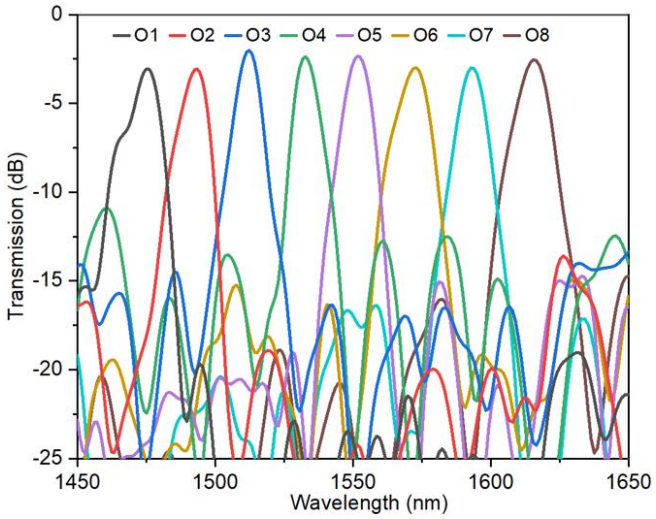

Fig. 3. The numerically simulated transmission spectra of the designed 8-channel wavelength demultiplexer.

demultiplexer is numerically simulated and shown in Fig. 3. The peak efficiency variations for different channels is consider as an optimization FOM. As seen from the flat top of the simulated spectra, a good balance between different wavelengths is achieved. The operating bandwidth of the device covers 1475 nm-1615 nm wavelength, and the wavelength channel spacing is estimated to be 20 nm, which meets the demand of coarse wavelength division multiplexing (CWDM) system at C communication band. The Insertion loss (IL) of the device is 2.2 dB, and the inter-channel crosstalk (CT) is below -10 dB.

Considering that it is very challenging to precisely control the fabricated dimension of the meta-structure because of the unavoidable and random fabrication imperfection in practice, the manufacturing tolerance is numerically investigated. Fig. 4(a) shows the simulated transmission spectra of the designed device with different nanohole-diameter. It can be seen that the peak wavelengths are consistently blue shifted when the nanohole diameter change from 90 nm to 110 nm.

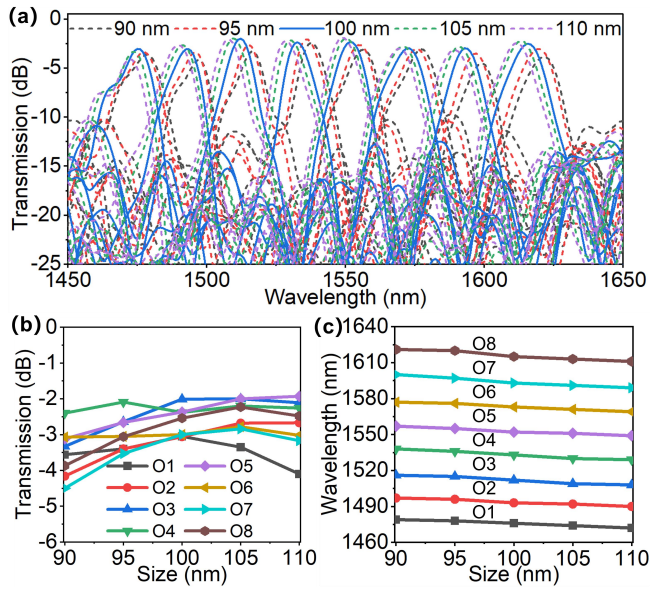

Fig. 4. The numerically simulated (a) transmission spectra, (b) ILs and (c) wavelength shift of the designed 8-channel wavelength demultiplexer with different nanohole-diameters.

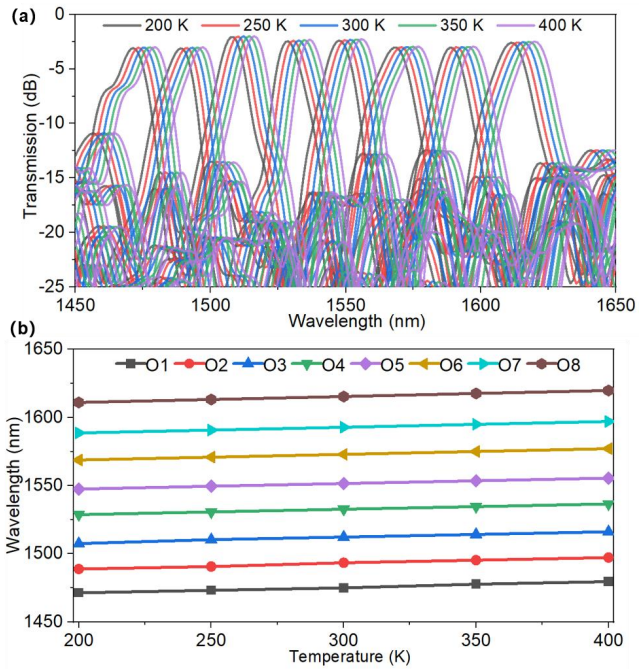

Fig. 5. The numerically simulated (a) transmission spectra and (b) wavelength shift of the designed 8-channel wavelength demultiplexer with different temperatures.

The dashed lines with different colors in the figure represent the transmission patterns when the sizes are different. Fig. 4(b) and (c) show the ILs and wavelength shift for all output channels with different nanohole-diameter. It can be seen that the ILs drop are within 1.5 dB, and the maximum wavelength-shift is 10 nm within the 20 nm diameter variation. The simulation results show that the designed device can maintain a good performance within ±5 nm pixel size variation.

The device performance may be affected by temperature change in practical application. We also theoretically simulate the device performance at different temperatures. When the temperature changes from 200 K to 400 K, the transmission spectra of the device is shown in Fig. 5(a). Different colors correspond to different temperatures. It can be seen that the ILs and CTs of the device can be maintained fairly well within the temperature change of 200K, and the peak wavelengths are consistently red shifted. The peak wavelength as a function of temperature is sampled and plotted in Fig. 5(b). It can be observed that the maximum wavelength-shift is ~15 nm. Therefore, our device has a good temperature robustness in the range of 100 K.

IV. Conclusion

In summary, we have proposed an ultra-compact eight-channel wavelength demultiplexer with 20 nm spacing and a footprint of 7.2×12 μm^2 via digitized meta-structure. The simulation peak insertion loss is 2.2 dB, and the crosstalk is <-10 dB. In addition, the simulation indicates that the device has good manufacturing and temperature tolerance. The designed wavelength demultiplexer is important in on-chip WDM systems for the ultra-dense integration.

Acknowledgment

This work is supported by National Natural Science Foundation of China (NSFC) (U21A20454), Shenzhen Science and Technology Innovation Commission (RCYX20210609103707009), Natural Science Foundation of Guangdong Province for Distinguished Young Scholars (2022B1515020057).

References

[1] Y. Liu, X. Wang, Y. Yao, J. Du, Q. Song, K. Xu, "Silicon photonic arrayed waveguide grating with 64 channels for the 2 μm spectral range," Opt. Lett., vol. 47, pp. 1186-1189, 2022.

[2] H. Xu, Y. Shi, "Flat-top CWDM (de)multiplexer based on MZI with bent directional couplers," IEEE Photon. Technol. Lett., vol. 30, pp. 169-172, 2017.

[3] T. H. Yen, Y. J. Hung, "Fabrication-tolerant CWDM (de)multiplexer based on cascaded Mach–Zehnder interferometers on silicon-on-insulator," J. Light. Technol., vol. 39, pp. 146-153, 2020.

[4] D. T. H. Tan, A. Grieco, Y. Fainman, "Towards 100 channel dense wavelength division multiplexing with 100 GHz spacing on silicon," Opt. Express, vol. 22, pp. 10408-10415, 2014.

[5] F. Wang, X. Xu, C. Zhang, C. Sun, J. Zhao, "Design and demonstration of compact and broadband wavelength demultiplexer based on subwavelength grating (SWG)," IEEE Photon. J., vol. 14, pp. 1-6, 2022.

[6] K. Wang, X. Ren, W. Chang, L. Lu, D. Liu, M. Zhang, "Inverse design of digital nanophotonic devices using the adjoint method," Photonics Res., vol. 8, pp. 528-533, 2022.

[7] Y. Liu, et al., "Arbitrarily routed mode-division multiplexed photonic circuits for dense integration," Nat. Commun., vol. 10, p. 3263, 2019.

[8] B. Shen, P. Wang, R. Polson, R. Menon, "An integrated-nanophotonics polarization beamsplitter with 2.4×2.4 μm^2 footprint," Nat. Photonics, vol. 9, pp. 378-382, 2015.

[9] A. Y. Piggott, J. Lu, K. G. Lagoudakis, J. Petykiewicz, T. M. Babinec, J. Vučković, "Inverse design and demonstration of a compact and broadband on-chip wavelength demultiplexer," Nat. Photonics, vol. 9, pp. 374-377, 2015.

[10] Y. Xu et al., "Inverse-designed ultra-compact high efficiency and low crosstalk optical interconnect based on waveguide crossing and wavelength demultiplexer," Sci. Rep., vol. 11, p. 12842, 2021.

[11] M. Yuan, G. Yang, S. Song, L. Zhou, R. Minasian, X. Yi, "Inverse design of a nano-photonic wavelength demultiplexer with a deep neural network approach," Opt. Express, vol. 30, pp. 26201-26211, 2022.

[12] L. Su, A. Y. Piggott, N. V. Sapra, J. Petykiewicz, J. Vuckovic, "Inverse design and demonstration of a compacton-chip narrowband three-channel wavelength demultiplexer," ACS Photon, vol. 5, pp. 301-305, 2018.

[13] J. Han, J. Huang, J. Wu, J. Yang, "Inverse designed tunable four-channel wavelength demultiplexer," Opt. Commun., vol. 465, 2020.